# A unified view of inorganic stereochemistry and stereochemical changes

Brian F.G. Johnson
*Department of Chemistry, The University of Edinburgh, West Mains Road, Edinburgh EH9 3JJ (UK)*

Alison Rodger
*Physical Chemistry Laboratory, South Parks Road, Oxford OX1 3QZ (UK)*

Susan M. Colwell
*University Chemical Laboratory, Lensfield Road, Cambridge CB2 1EW (UK)*

(Received November 15, 1993; revised January 21, 1994)

**Abstract**

Relationships between geometries adopted by compounds, $ML_n$, with different coordination numbers are developed and stereochemical changes in coordination compounds are analysed in terms of these relationships. The atom–atom interaction model (AAIM) view of molecular geometry in covalent species $ML_n$ is used to quantify the discussion where required. The AAIM emphasises the importance of both M–L bond and L–L interaction energies.

*Key words:* Stereochemistry; Atom–atom interaction model; Coordination compounds

## 1. Introduction

The classic valence shell electron pair repulsion scheme (VSEPR) [1] has been used with outstanding success as a simple guide to the stereochemistry of inorganic molecular compounds, but its application is limited because of its reliance on the stereochemical consequences of lone pairs of electrons. The attractive feature of VSEPR, namely, that detailed quantum calculations [2] are not required for each system studied, is retained by an alternative approach originally developed by Bartell [3] for organic systems and later extended by Glidewell [4]. In this approach, the geometry of a molecule, $ML_n$, is interpreted in terms of a 'non-bonded' radius for an atom or group of atoms, L. It has achieved considerable success in the evaluation of bond angles and distances and has also been successfully applied to the prediction of rotational barriers in certain organic systems. Hyde [5] has developed a similar model for the study of crystals.

One of the main attractions of these atom–atom approaches to molecular geometry is that they enable geometries to be visualised and the energetic consequences of stereochemical changes to be readily determined. We have previously developed a model [6], the atom–atom interaction model (AAIM), for determining molecular geometry which extends the non-bonded radii approaches to include attractive interactions. The Bartell–Glidewell non-bonded radius defines the minimum distance between two atoms, with the magnitude of the non-bonded radius being due to the short range repulsion of overlapping electron clouds. Whether or not two atoms in a molecule are separated by that distance depends on the balance of all the repulsive and attractive forces between non-bonded atoms, subject to any constraints imposed by the bonds within the molecule.

There are instances where bond strengths are significantly dependent upon the relative orientation of the ligands about the atom. In such cases, the ligand–ligand interactions do not dominate the geometry adopted by the molecule. The simplest case of this kind is $BeH_2$ which would be bent if dominated by ligand–ligand attraction, but is in fact linear as the BeH bonds are far stronger for this geometry [6]. In this work, we assume bond strength is independent of orientation. However, it should be noted that we are not ignoring all electronic effects, since the ligand–ligand interactions are also determined by electrons. For transition metal complexes, although the influence of elec-


*SSDI* 0020-1693(94)03841-B

tronic factors in, for example, $d^8$ systems is well-established, they tend to determine the coordination number rather than dominate the ligand orientations. However, the underlying assumption of constant bond strengths must be remembered for all situations where the metal electron structure is not spherical.

For practical purposes the AAIM is closely related to molecular mechanics, the main differences being that twist and bond angle force constants are not explicitly considered. Due to the flexibility of bonding modes for transition metals these omissions are usually not a problem for transition metal complexes [7]. The omission of bond angle constraints is, on the other hand, a positive advantage if one wishes to study reactions rather than only stable geometries, since the bond angle force constants are defined for the known stable reactants and products. Within the AAIM, the L–L non-bonded interactions account for the bond angle force constants of molecular mechanics. Application of the AAIM to reaction mechanisms is reported in ref. 8.

The aim of this work is to develop a unified view for approaching two questions: (i) why do some molecules adopt stable geometries which differ, to a greater or lesser extent, from the most regular shape possible for a given coordination number? and (ii) is there is a dominant factor determining the stereochemical changes – fluxionality and isomerisation – that many inorganic coordination complexes exhibit? In Section 2, a brief discussion of the structural implications of varying ligand or metal sizes are discussed. Since metal size and M–L bond length are related, this discussion leads directly to the analysis of reactivity in Section 3.

## 2. $ML_n$ stable geometries

Within the AAIM, the stereochemistry of a covalent molecular species $ML_n$ is seen to be governed primarily by the need to achieve the optimum M–L bond distances and, secondly, by the need to maximise the L–L attractive interactions subject to short range repulsions. Thus for small M (or equivalently short M–L bonds), the ligands will pack around M in a close-packed *closo* geometry with triangular or deltahedral faces. Now let the size of M (or equivalently, the M–L bond length, $d$(M–L), increase, with the ligands remaining the same size. If the molecule is forced to retain its original shape, then each L–L distance, $d$(L–L), increases, with a resultant loss of L–L dispersive stabilisation. If the ligand polyhedron is then allowed to relax, it will adopt the geometry which maximises (the number of) attractive L–L interactions subject to the short range repulsive interaction [6a]. This means that the ligand polyhedron relaxes by breaking the L–L edge which allows maximum relaxation of the ligand system for minimum loss of nearest neighbour contacts. One square face is created in the process.

This process can be readily visualised when one realises that the same relaxation is required for the insertion of a new vertex (of connectivity four) along an edge of the ligand polyhedron to form a new polyhedron. For polyhedra whose internal angles are less than 180°, the edge that allows most relaxation is one which is 'opposite' one, or preferably two, vertices of lowest connectivity, where connectivity refers to the number of nearest neighbours. By opposite we mean that when the edge is broken, the one or two lowest connectivity vertices are part of the square face, but were not previously connected by the broken edge. The resulting ligand polyhedron for $ML_n\eta$ (where $\eta$ denotes hole) is a *closo*-$(n+1)$ vertex polyhedron. These are illustrated in Fig. 1. The relaxation to the next *closo*-polyhedron has the additional advantage of reducing the longest M–L distances (L of lowest connectivity are always furthest from M (see Table 1)). The $ML_{11}$ ligand polyhedron differs from the above picture since it is only slightly distorted from the regular icosahedron, and so relaxation after expansion will be towards a regular icosahedron with a hole. (It should be noted that the polyhedral forms adopted by the metal or boron atoms cluster compounds [9] are not necessarily the same as those adopted by the ligands of complexes since the energetic considerations are different.)

For larger increases in M size or M–L bond length, the relaxation can be viewed as the sequential cleavage of polyhedral edges by following the sequence in Fig. 1 for two or more steps so inserting two or more interstitial holes. The choice of second, third etc. insertion point relative to holes already present must be the one allowing greatest relaxation. For convenience we shall refer to a *closo*-polyhedron with $n$ vertices as $\{n,0\}$, a *nido*-polyhedron as $\{n,-1\}$, and an *arachno*-polyhedron as $\{n,-2\}$, etc. Thus the hole created in going from *nido*-$\{n+1,-1\}$ to *arachno*-$\{n+2,-2\}$ may not be the same as for *closo*-$\{n+1,0\}$ to *nido*-$\{n+2,-1\}$. For example, one edge of the *closo*-tetrahedron is broken to form the butterfly *nido*-trigonal bipyramid and a second edge broken to form the square plane *arachno*-octahedron rather than the butterfly. This sequence may be expressed as $\{4,0\}\rightarrow\{5,-1\}\rightarrow\{6,-2\}$ (Fig. 2). Further relaxation to $\{7,-3\}$ results in a pyramidal shape which would be further stabilised by relaxation to a square pyramid with equal $d$(M–L). It should be noted, however, that when the number of holes is not small relative to $n$, the uniqueness and accuracy of the description is lost, and is probably unhelpful. These stages are illustrated in Fig. 3. Analogous relaxation processes are also illustrated in Fig. 2 for $\{3,0\}$ and $\{5,0\}$.

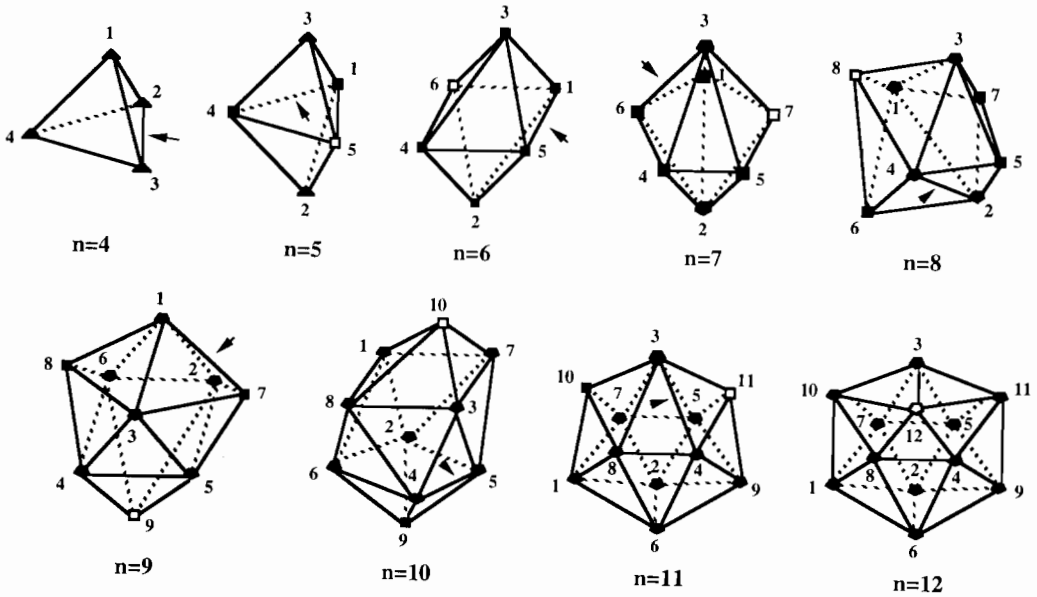


Fig. 1. $MX_n$ geometries for $n=4$–12. The arrows indicate the L–L edge or insertion point that leads to greatest relaxation. The open square in each diagram is the interstitial hole resulting from insertion into the previous *closo*-polyhedron. Vertices are labelled consistently from polyhedron to polyhedron and the polygon drawn at each vertex indicates the number of its nearest neighbours.

TABLE 1. M–L bond lengths for *closo*-$ML_n$, $n=3$–10 and 12, taking the ligand hard sphere radius to be half a unit of length and the ligands to be close packed. Subscripts denote the L–L connectivity of the ligand

| | $d_2$ | $d_3$ | $d_4$ | $d_5$ |
|---|---|---|---|---|
| $ML_3$ | 0.577 | | | |
| $ML_4$ | | 0.612 | | |
| $ML_5$ | | 0.816 | 0.577 | |
| $ML_6$ | | | 0.707 | |
| $ML_7$ | | | 0.851 | 0.526 |
| $ML_8$ | | | 0.930 | 0.677 |
| $ML_9$ | | | 0.995 | 0.764 |
| $ML_{10}$ | | | 0.995 | 0.764 |
| $ML_{12}$ | | | | 0.951 |

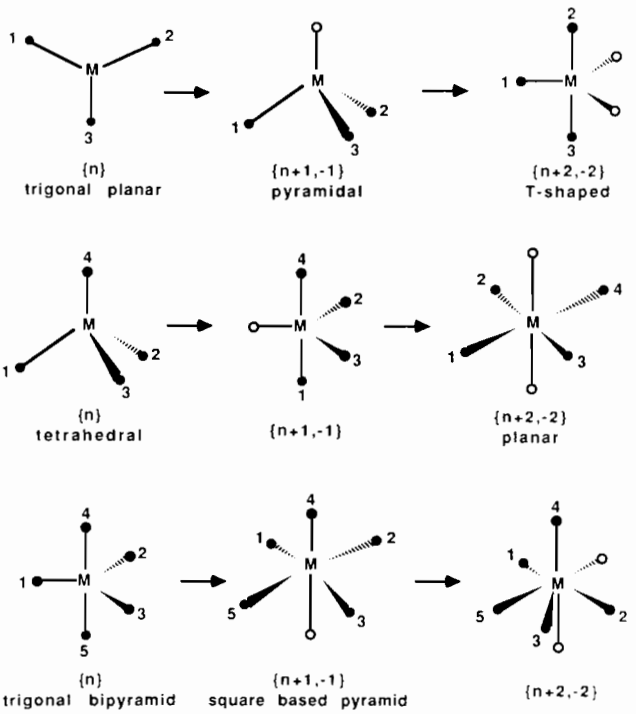


Fig. 2. $MX_n$ geometries for $n=3$, 4, 5. Solid circles indicate atoms and open circles vacant sites resulting from the expansion of the ligand polyhedron and subsequent relaxation.

The octagonal {6,0} and trigonal prismatic $\{9,-3\}$ are the commonly expected six-coordination geometries [10]. The 'expansion' sequence for $ML_6$ is illustrated in Fig. 3. Outside the context of this discussion, there appears no mention in the literature of the *nido*-7 pentagonal bipyramid nor the *arachno*-8 triangulated dodecahedron as possible six-coordinate geometries although they are obliquely referred to in several discussions. The $ML_6$ series does not necessarily end at the trigonal prism $\{9,-3\}$, but may proceed to $\{10,-4\}$ etc. However, such structures are only to be expected for the very largest cations and the very smallest ligands.

For seven coordination the *closo*-polyhedron {7,0} is the pentagonal bipyramid, $\{8,-1\}$ corresponds to the capped octahedron (consider the $ML_8$ structure of Fig. 1, and draw a line between the two five-fold vertices across the empty vertex, this is then the standard representation of a capped octahedron [10]), and $\{9,-2\}$ the monocapped trigonal prism. Similarly, for eight coordination we would expect the first three members of the series for $ML_8$ to correspond to the dodecahedron

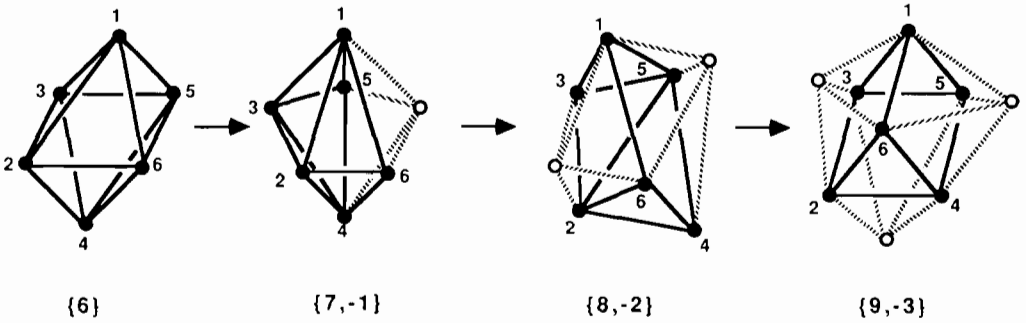


Fig. 3. $MX_6$ geometries. Solid circles indicate atoms and open circles vacant sites resulting from the expansion of the ligand polyhedron and subsequent relaxation.

{8,0}, the bicapped trigonal prism $\{9,-1\}$ and the square antiprism $\{10,-2\}$.

This discussion has direct relevance for geometries of molecules where M changes down the periodic table. Thus Ni complexes are almost always tetrahedral, but Pt ones are often square planar. In practice, intermediate geometries such as 'distorted tetrahedral' may be observed (see data in ref. 6a). Similarly, as ligands decrease in size, for example, changing I for Br, such changes are expected. The most significant importance of these ideas, however, is for transition metal complex reactivity, especially of *closo* geometries.

## 3. Stereochemical changes

The stereochemical changes – fluxionality and isomerisation – that many inorganic coordination compounds exhibit has become one of the most widely studied phenomena in inorganic chemistry and although the mechanisms of some, for example, rearrangement processes in five-coordination [11] or six-coordination [7a,b, 10] complexes, are well understood, no simple coherent approach to all coordination numbers appears to have evolved. By applying the discussion of Section 2 to rearrangement mechanisms we shall develop an approach to this problem which we believe offers a more unified view of these fascinating phenomena.

A *closo* ligand polyhedron $\{n,0\}$ has the ligands in contact, so it cannot rearrange without stretching M–L distances. So, imagine the reaction of a *closo* polyhedron proceeding by first the M–L bonds stretching, followed by relaxation of $\{n,0\}$ to $\{n+1,-1\}$ as discussed in Section 2. If $\{n+1,-1\}$ can relax back to a 'new' $\{n,0\}$ polyhedron – new in the sense that if the atoms could be labelled it would be apparent that different atoms are in different positions – then $ML_n$ can rearrange by a mechanism of simultaneous bond stretching and ligand relaxation to a transition state $\{n+1,-1\}$, and subsequent relaxation to the new polyhedron. The Berry pseudo rotation of trigonal bipyramidal systems is an example of such a process [11]. Frequently, however, $\{n+1,-1\}$ cannot relax to a new $\{n,0\}$. In this case, further M–L bond stretching and ligand relaxation to $\{n+2,-2\}$ may be sufficient. The rearrangement of tetrahedral complexes via a square planar structure [12] is an example of this. Octahedral (or more commonly tris-chelate) rearrangements via a trigonal prismatic transition state [7a,b, 13] is an example of reaction via an $\{n+3,-3\}$ transition state.

Non-*closo* polyhedra *may* rearrange via the same mechanism as their *closo* analogues. However, before drawing such a conclusion, mechanisms proceeding via less open ligand geometries must be considered. For example, a square planar $ML_4$ $\{6,-2\}$ may change to a $\{5,-1\}$ ligand polyhedron with no decrease in M–L bond strength only loss of favourable dispersive L–L interactions. This is generally energetically less expensive than bond stretching, so if a $\{6,-2\}$ polyhedron can rearrange via $\{5,-1\}$ or $\{4,0\}$ rather than via, say, $\{7,-3\}$ then it will. In this case, however, neither of these ligand motions leads smoothly to a new square planar structure, so a square planar compound must follow the trigonal twist mechanism of its octahedral template [8d]. (A mechanism going from $\{6,-2\}$ to $\{4,0\}$ could then lead to a new $\{6,-2\}$ but not with the same vibration.) By way of contrast, a $\{5,-2\}$ T-shaped $ML_3$ can rearrange via $\{3,0\}$ without stretching M–L bond lengths.

Consideration of a limited number of examples led us to postulate that rearrangements of *closo*-$ML_n$ that could proceed via a transition state $\{n+1,-1\}$ are likely to be fluxional, and those proceeding via $\{n+2,-2\}$, $\{n+3,-3\}$ etc. become less likely until a bond breaking mechanism is more favourable. Similarly, non-*closo*, $\{n,-i\}, i>0$, structures will be fluxional if their transition states are either $\{n+1,-i-1\}$, so involving only slight stretching of the M–L bonds, or $\{n-k,-i+k\}$ $k>1$, which involves no M–L bond stretching merely loss of L–L attractive interactions. Thus, rearrangement mechanisms for $ML_n$ systems can be visualised as proceeding in the stages indicated by the geometry distortion

schemes of Section 2. A given molecule proceeds as far along the scheme as is necessary to reach a geometry that can relax to a new product (rather than only back to the reactant). In practice, each reaction *step* may involve two or more *stages* of the Scheme. Thus for example the Bailar twist is a concerted mechanism that can be visualised using Fig. 3 as occurring in three stages to the transition state and three to the product. Alternatively, one or more of the stages may in fact be steps along the rearrangement pathway (with, for example, $\{8,-2\}$ being an intermediate).

If this view of rearrangement mechanisms is correct, it must be consistent with the previously derived classical symmetry selection rule procedure for reaction mechanisms [14]. In particular, the distortion postulated to lead to rearrangement must be a normal coordinate for a particular molecular geometry (not necessarily a stable species). By this we mean, when mass weighted coordinates are used, it uncouples the kinetic and potential energies of the system and diagonalises the potential energy. Thus at the reactant, the very beginning of the motion towards the next polyhedron must be a normal coordinate of the reactant in the usual sense of the term. At each subsequent point, the normal coordinates must be re-evaluated – the reactant normal coordinates will not be appropriate part way towards the transition state. However, as the reactant normal coordinates will continuously transform into those of the transition state, it is generally the case that if the route via a particular transition is energetically feasible, then the beginning of the distortion from $\{n,0\}$ must be one of the lower energy normal modes of the reactant, $\{n,0\}$. We have therefore determined the normal modes [15] of $ML_n$ for $n=4$–11, and also the projection of the $\{n,0\}$ to $\{n+1,-1\}$ motion onto each normal mode of $\{n,0\}$. Although the relative orderings of the normal modes vary as a function of the M–L bond strength, in each case the mode which resembles the $\{n,0\}$ to $\{n+1,-1\}$ motion most closely is one of the three lowest energy vibrational normal modes.

The M–L bond stretch required for each stage in a reaction scheme (as opposed to each step) is another indication of the energy required for a proposed mechanism. The stretches can be deduced from Table 1, where the M–L bond lengths for $ML_n$ are determined assuming close-packed hard sphere ligands of radius 1. Thus, for example, $ML_6$ rearranging via a trigonal prism $\{9,-3\}$ requires the M–L bonds to stretch by 8%. The corresponding volume change, or activation volume, assuming the ligands are close packed in both reactant and transition state is $[\sqrt{6}r^3/2-2r^3/3]$ where $r$ is the reactant M–L distance. We can compare this result with an experiment for $[Cr(1,10\text{-phenanthroline})_3]^{3+}$ and $[Cr(2,2'\text{-bipyridyl})_3]^{3+}$ which are known to react via a twist mechanism. Since $r=2.07$ Å [16] for these molecules, and assuming that the ligands take up the same volume in the reactant and the transition state so that the experimental activation volume is due only to changes in the metal-ligating atom part of the molecule, the molar activation volume is predicted by the AAIM to be 3.0 $cm^3$. The experimental value is $3.3\pm0.3$ $cm^3$ [17].

The utility of our approach for the study of the geometry and isomerisation reactions of $ML_n$ molecules increases with the number of ligands since it enables apparently complex geometries to be simply systematised. For seven coordination, there is no single-stage route to a new molecule available: single edge cleavage leads to a *nido*-8 vertex polyhedron, $\{8,-1\}$ (see Fig. 1) which can only relax to a capped octahedron with one significantly stretched M–L bond. A further edge cleavage is required to give the more favourable *arachno*-tricapped trigonal prism, $\{9,-2\}$, which can serve as a transition state. Hence the probably concerted ligand rearrangement for a pentagonal bipyramid can be viewed as taking place by a five stage process:

$$\{7,0\} \longrightarrow \{8,-1\} \longrightarrow \{9,-2\} \longrightarrow \{8,-1\}' \longrightarrow \{7,0\}'$$

Such a motion corresponds to a soft (i.e. low energy) vibrational mode.

For eight coordination we have a situation similar to that found for coordination number five. The parent polyhedron is the dodecahedron $\{8,0\}$. Single edge cleavage takes it to the bicapped trigonal prism, $\{9,-1\}$, which can clearly serve as a suitable transition state geometry since further extension along the same vector leads to a new dodecahedron $\{8,0\}'$. Thus rearrangement is a two stage concerted process

$$\{8,0\} \longrightarrow \{9,-1\} \longrightarrow \{8,0\}'$$

It is interesting to note that, $\{6,0\}$, $\{7,0\}$ and $\{8,0\}$ all proceed via the same polyhedral intermediate, just as $\{3,0\}$, $\{4,0\}$ and $\{5,0\}$ all proceed via the octahedron.

## 4. Conclusions

In summary what we have shown is that there is a coherent way of viewing the apparently disparate geometries adopted by transition metal complexes both at equilibrium and during the course of isomerisation reactions. Three factors are important in determining the geometry of a system: (i) the short range L–L repulsion (which can for simplicity be conceptually viewed in terms of hard sphere repulsion), (ii) the M–L bond lengths, (iii) the longer range L–L attraction due to dispersive interactions. If one were to build a transition metal complex from component atoms, one would therefore first ensure that the ligands are not forced so close together that their hard spheres are overlapping,

then try to set metal–ligand bond lengths close to the value that maximises the bond strength, and finally orient the ligands around the metal so that as many as possible of the ligand hard spheres touch or nearly touch. Although it is the smallest energy contribution, the ligand–ligand attraction often has a significant effect on the appearance of the complex. When considering isomerisation pathways, the L–L interactions become even more important as they dictate how the geometry of the ligand system relaxes to the change in the bond lengths that occur during the reaction. Minimal loss of dispersion energy results if the minimum number of L–L contacts are broken. Thus the bond stretching/ligand polyhedron relaxation can be viewed as proceeding along the stages of Figs. 2 and 3, from the starting ligand polyhedron to one where the ligands are once more in contact but with longer M–L bond lengths. The relaxation can be equivalently viewed as the insertion of interstitial holes along the edges of the expanded reactant polyhedron that allow maximum relaxation. By coupling the AAIM analysis with a normal mode analysis one is then in a position to examine both concerted and non-concerted rearrangement mechanisms of transition metal complexes.

For high symmetry $\{n,0\}$ polyhedra, e.g. the tetrahedron, the octahedron and the cube (and incidentally the icosahedron and the pentagonal dodecahedron), the distortion towards the *nido*-$\{n+1,-1\}$ polyhedron may be difficult to observe experimentally. Consider, for example, an octahedral complex. Since all L–L contact distances are equal, distortion may occur along any one of the twelve equivalent edges. However, because certain experimental methods, for example, X-ray analysis, provide only a time-averaged structure, a structure with average $O_h$ symmetry may be recorded. Vibrational spectroscopy, however, with a much shorter time scale, can provide information relevant to the proposed distortion towards the *nido*-pentagonal bipyramid. For example, the vibrational spectrum of $[TeX_6]^{2-}$ is interpreted in terms of large amplitude and abnormal frequencies suggesting that the octahedral geometry is rather tenuously stable, i.e. the molecule is 'floppy' [18] and moving, according to our view, towards a $\{7,-1\}$ geometry. For $XeF_6$ the geometry of the gas-phase molecule is non-octahedral and the species is flexible, having a near-zero force constant for one of the bending modes of the octahedron, which is again consistent with a *nido*-$\{7\}$ geometry.

## Acknowledgements

A.R. acknowledges the support of the Glasstone Trust and the helpful comments of the referees.

## References

1 R.J. Gillespie and R.S. Nyholm, *Q. Rev., 11* (1975) 339.
2 W.J. Hehre, L. Radom, P.V.R. Schleyer and J.A. Pople, *Ab Initio Molecular Orbital Theory,* Wiley, Australasia Pty. Ltd., Sydney, 1971.
3 L.S. Bartell, *J. Chem. Phys., 32* (1960) 827.
4 C. Glidewell, *Inorg. Chim. Acta, 12* (1975) 219.
5 G. Hyde, *J. Proc. R. Soc. N.S.W., 119* (1986) 153.
6 (a) A. Rodger and B.F.G. Johnson, *Inorg. Chim. Acta, 146* (1988) 35; (b) D. Braga, A. Rodger and B.F.G. Johnson, *Inorg. Chim. Acta, 174* (1990) 185.
7 M. Drew, personal communication, 1990.
8 (a) A. Rodger and B.F.G. Johnson, *Inorg. Chem., 27* (1988) 3061–3062; (b) B.F.G. Johnson and A. Rodger, *Inorg. Chem., 28* (1989) 1003–1006; (c) A. Rodger and B.F.G. Johnson, *Polyhedron, 8* (1989) 1742–1744; (d) A. Rodger, *Inorg. Chim. Acta, 185* (1991) 193–200.
9 K. Wade, *Chem. Br., 11* (1975) 177.
10 J.K. Burdett, *Molecular Shape,* Wiley, New York, 1980, p. 24; W.W. Porterfield, *Inorganic Chemistry: A Unified Approach,* Addison Wesley, Reading, MA, 1984.
11 S.J. Berry, *Chem. Phys., 22* (1960) 933.
12 A. Rodger and P.E. Schipper, *Inorg. Chem., 27* (1988) 458.
13 J.R. Hutchison, J.G. Gordon and R.H. Holm, *Inorg. Chem., 10* (1975) 1004, and refs. therein.
14 A. Rodger and P.E. Schipper, *Chem. Phys., 107* (1986) 329; *J. Phys. Chem., 91* (1987) 189.
15 M. Born and K. Huang, *Dynamical Theory of Crystal Lattices,* Oxford University Press, Oxford, 1968.
16 G. Orpen, L. Brammer, F.H. Allen, O. Kennard, D.G. Watson and R. Taylor, *J. Chem. Soc., Dalton Trans.,* (1989) S1–S83.
17 R. van Eldik (ed.), *Inorganic High Pressure Chemistry. Kinetics and Mechanism,* Elsevier Science, Amsterdam, Netherlands, 1986.
18 C.J. Adams and A.J. Downs, *Chem. Commun.,* (1970) 1699.